Jet Results in pp and Pb-Pb Collisions at ALICE

Oliver Busch for the ALICE collaboration
Universität Heidelberg, Physikalisches Institut, Heidelberg, Germany

We report results on jet production in pp and Pb-Pb collisions at the LHC from the ALICE collaboration. The jet cross section in pp collisions at $\sqrt{s}$=2.76 TeV is presented, as well as the charged particle jet production cross section and measurements of the jet fragmentation and jet shape in pp collisions at $\sqrt{s}$=7 TeV. NLO pQCD calculations and simulations from MC event generators agree well with the data. Measurements of jets with a resolution parameter R=0.2 in Pb-Pb collisions at $\sqrt{s_{NN}}$=2.76 TeV show a strong, momentum dependent suppression in central events with respect to pp collisions. The centrality dependence of the suppression of charged particle jets relative to peripheral events is presented. The ratio of jet spectra with R=0.2 and R=0.3 is found to be similar in pp and Pb-Pb events. The analysis of the semi-inclusive distribution of charged particle jets recoiling from a high-$p_{\rm T}$ trigger hadron allows an unbiased measurement of the jet structure for larger cone radii.

1 Introduction

Jets are collimated sprays of particles associated with hard scattered partons. The study of jet production and fragmentation allows us to test our understanding of perturbative and non-perturbative aspects of QCD. In heavy-ion collisions, jets produced in the initial stage probe the hot and dense nuclear matter created during the quark gluon plasma phase of the fireball evolution. Interactions with the medium give rise to additional induced radiation. Jet reconstruction aims to capture the full dynamics of jet quenching and to quantify the in-medium jet energy loss.

2 Data analysis

Charged jets are reconstructed in the ALICE central barrel from primary charged particle tracks measured in the Inner Tracking System (ITS) and the Time Projection Chamber (TPC). Tracks with transverse momentum $p_{\rm T} > 150$ MeV/c in the pseudo-rapidity interval $|\eta| < 0.9$ are clustered with the FastJet [1] anti-$k_{\rm T}$ algorithm using a boost invariant $p_{\rm T}$ recombination scheme. We use different values of the jet resolution parameter from R=0.2 to R=0.4. Jets are selected so that they are fully contained within the detector acceptance. For full jet reconstruction, we include neutral particles (mostly neutral pions) reconstructed with the ALICE Electromagnetic Calorimeter (EMCal). Clusters in the EMCal acceptance $|\eta| < 0.7$ and $1.4 < \varphi < \pi$ with a transverse energy $E_{\rm T} > 300$ MeV are used. The energy of charged particles pointing to EMCal clusters is subtracted to avoid double-counting. The jet shape and jet constituents' transverse momentum spectra (jet fragmentation) are measured with charged particles in the leading (highest $p_{\rm T}$) jet in each event. The jet spectra, shape, and fragmentation distributions are corrected for detector effects (including the missing energy from e.g. neutrons and K^0_L in the measurements that include the EMCal) via unfolding or bin-by-bin corrections based on detector simulations.

Jet reconstruction in heavy-ion collisions proceeds against a large background from the underlying event uncorrelated to hard parton scattering. The average charged background energy density is evaluated event by event from the median p_{T} density of FastJet [1] k_{T} clusters and subtracted jet by jet. For charged+EMCal jet reconstruction, the charged background density is scaled to the level of charged+neutral particles. The spectra are corrected for detector effects and background flucutations via unfolding.

3 Results from pp collisions

In the top-left panel of Fig. 1, we present the inclusive differential jet cross sections [2] in pp collisions at $\sqrt{s}$=2.76 TeV, measured using charged+neutral particles. The data are compared to NLO pQCD results [3,4]: good agreement is found when hadronization effects are applied to the perturbative calculations.

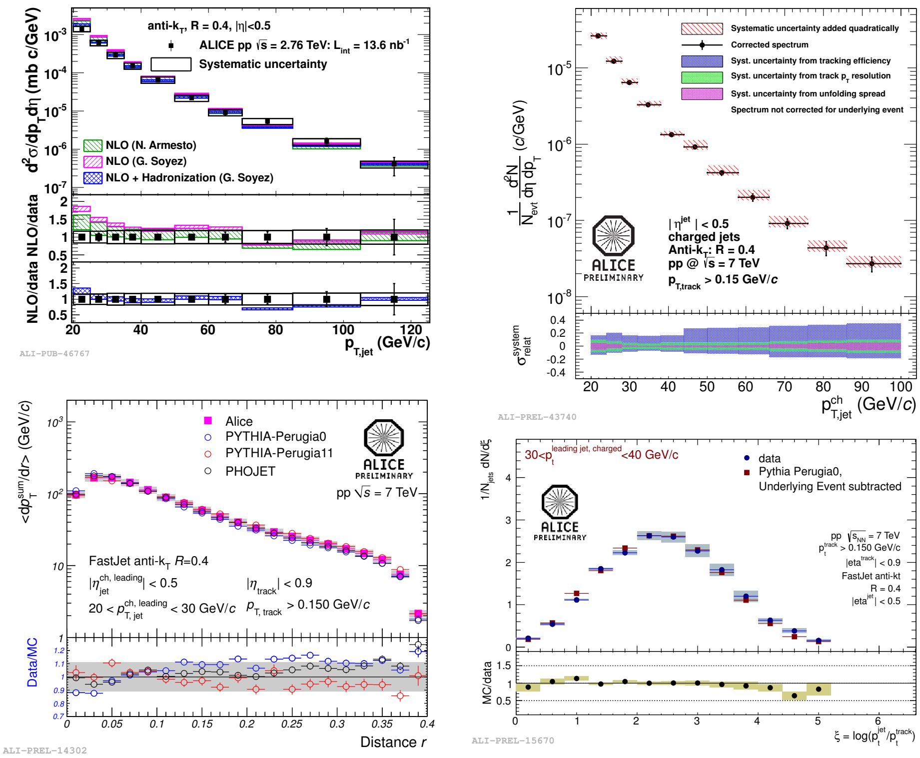

Figure 1: Results from pp collisions at $\sqrt{s}$=2.76 TeV and 7 TeV. Top left: inclusive differential jet cross section for R=0.4 at $\sqrt{s}$=2.76 TeV. Boxes show the systematic uncertainty. The data are compared to NLO pQCD calculations indicated by the bands, ratio of calculations to data are shown in the lower panel. Top right: charged jet cross section for R=0.4 at $\sqrt{s}$=7 TeV. Systematic uncertainties are indicated by the boxes, the lower panel shows the contributions from detector effects and unfolding superimposed linearly. Bottom left: radial distribution of transverse momentum density measured in leading charged jets with $20 < p_{\mathrm{T,jet}}^{\mathrm{ch}} < 30$ GeV/c. Bottom right: scaled transverse momentum distribution of jet fragments for $30 < p_{\mathrm{T,jet}}^{\mathrm{ch}} < 40$ GeV/c. Jet shape and fragmentation distributions are compared to from calculations from PYTHIA (tunes Perugia0 and Perugia2011) and Phojet MC event generators.

In the top-right panel of Fig. 1, the charged jet cross section [5] at $\sqrt{s}$=7 TeV is shown. The bottom-left panel of Fig. 1 presents the leading charged jet shape [7] distribution of particle p_{T} sum in radial slices relative to the jet axis. The slope of the distribution measures the jet collimation. The fragmentation spectrum of scaled transverse momentum $\xi = \ln(p_{\mathrm{T}}^{jet,ch}/p_{\mathrm{T}}^{particle})$ for the charged jet constituents [8] shown in the bottom-right panel exhibits the characteristic hump-backed plateau structure indicating QCD coherence. The area of the distribution is equal to the charged particle multiplicity of the fragments. The measured jet shape and fragmentation are compared to MC simulations from the PYTHIA [9] (tunes Perugia0 and Perugia2011) and Phojet [10] event generators. The pp underlying event contribution was measured inside perpendicular cones transverse to the jet axis and subtracted from the jet cross section, fragmentation and shape measurements, consistently in data and simulations. The data are reasonably well described by the simulations.

4 Jets in Pb-Pb Collisions

Figure 2 shows the single inclusive jet cross section results [11,12] in Pb-Pb collisions at $\sqrt{s_{NN}}$ = 2.76 TeV. In the top-left panel we present the charged+EMCal jet spectrum for R=0.2 for the 10% most central events. Minimum transverse momentum, $p_{\mathrm{T}} > 5$ GeV, is required for the leading charged constituent. In the top-right panel the jet nuclear modification factor R_{AA} is shown, defined as the ratio of the measured jet spectra in Pb-Pb collisions to the pp reference scaled by the number of binary collisions [15]: $R_{\mathrm{AA}}(p_{\mathrm{T}}) = \frac{1}{\langle N_{\mathrm{coll}} \rangle} \frac{\mathrm{d}^2 N_{\mathrm{jet}}/\mathrm{d}p_{\mathrm{T,jet}}\,\mathrm{d}\eta}{\mathrm{d}^2 N^{\mathrm{pp}}_{\mathrm{jet}}/\mathrm{d}p_{\mathrm{T,jet}}\,\mathrm{d}\eta}$. The measured R_{AA} is significantly smaller than unity, indicating a strong suppression of jets in Pb-Pb collisions. The suppression is strongest at low jet momentum, at high momentum R_{AA} rises to values of the order of 0.5. The centrality dependence of the quenching is investigated via the charged jet R_{CP}, a quantity conceptually similar to R_{AA}, but using peripheral Pb-Pb events as a reference. R_{CP} [13,14] is presented in Fig. 2 in the bottom-left panel for 3 different centrality intervals. The suppression is seen to increase with centrality (lower R_{CP} values), and a more pronounced momentum dependence can be observed. In the bottom-right panel, we show, for two centrality classes, the ratio of the charged jet spectra obtained for R=0.2 to R=0.3. The ratio is sensitive to the jet structure. The measured ratio is consistent with the PYTHIA values for peripheral and central events: no broadening of the hard core of the reconstructed jets is observed within the present systematic uncertainties.

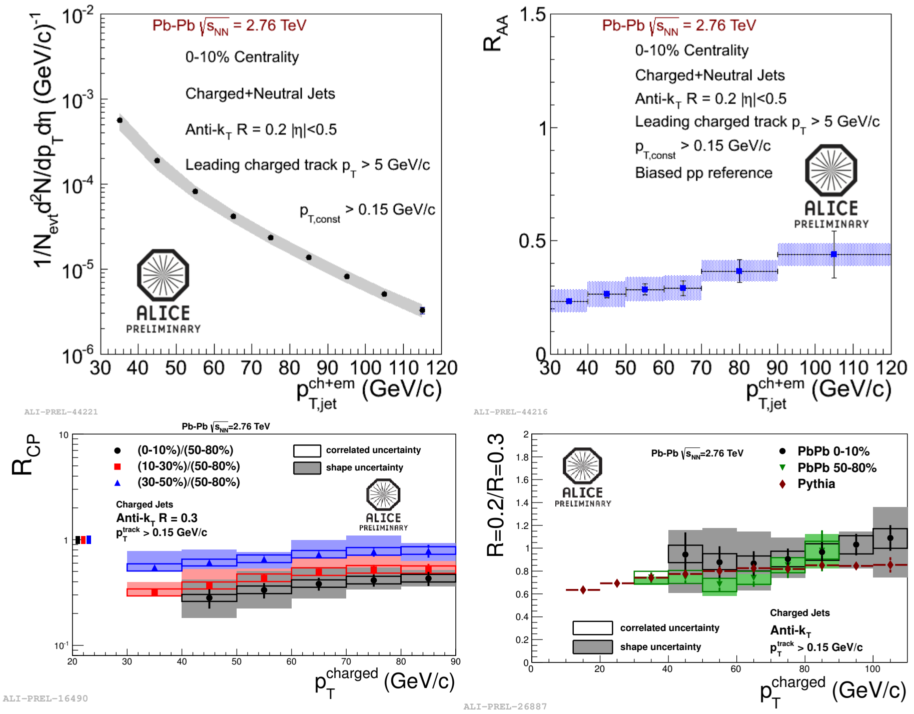

Figure 2: Single inclusive jet measurements in Pb-Pb collisions at $\sqrt{s_{NN}}$ = 2.76 TeV. Top left: inclusive jet spectrum for R=0.2 in the 10% most central events, with a 5 GeV/c fragmentation bias on the leading jet constituent. Systematic uncertainties are indicated by the shaded band. Top right: nuclear modification factor for R=0.2 biased jets in 0-10% central events. Bottom left: nuclear modification factor R_{CP} for charged jets with R=0.3 for different centrality selections. Bottom right: ratio of charged jet spectra with radius parameter R=0.2 and R=0.3 in central and peripheral Pb-Pb events, compared to PYTHIA calculations.

5 Hadron triggered recoil jets in Pb-Pb

The analysis of hadron triggered recoil jets allows us to extend the study of jet quenching to larger values of R. The semi-inclusive distribution of charged jets recoiling back-to-back from a high-pt charged hadron in Pb-Pb collisions [16] is measured. Constructing the difference spectra for different intervals of trigger hadron p_{T}, we subtract the contribution of combinatorial jets uncorrelated to the hadron trigger:

$$\Delta_{recoil}((p_{\mathrm{T}}^{\mathrm{trig},1}-p_{\mathrm{T}}^{\mathrm{trig},2})-(p_{\mathrm{T}}^{\mathrm{trig},3}-p_{\mathrm{T}}^{\mathrm{trig},4}))=\frac{1}{N_{\mathrm{trig}}}\frac{\mathrm{d}N}{\mathrm{d}p_{\mathrm{T,jet}}^{\mathrm{ch}}}(p_{\mathrm{T}}^{\mathrm{trig},1}<p_{\mathrm{T}}^{\mathrm{trig}}<p_{\mathrm{T}}^{\mathrm{trig},2})-c\frac{1}{N_{\mathrm{trig}}}\frac{\mathrm{d}N}{\mathrm{d}p_{\mathrm{T,jet}}^{\mathrm{ch}}}(p_{\mathrm{T}}^{\mathrm{trig},3}<p_{\mathrm{T}}^{\mathrm{trig}}<p_{\mathrm{T}}^{\mathrm{trig},4})$$

The Δ_{recoil} spectrum for R=0.4 is shown in the left panel of Fig. 3 for hadron trigger intervals from 20-50 GeV/c and 15-20 GeV/c, using a scale factor $c = 0.956$. This novel variable allows us to study an unbiased sample of jets reconstructed with a large radius, maintaining a jet constituent cutoff as low as $p_{\mathrm{T}}^{\mathrm{const}} > 0.15$ GeV/c.

To explore the energy redistribution within recoil jets, we consider the ratio for the measured Δ_{recoil} distribution over PYTHIA (tune Perugia 2010) simulations ΔI_{AA}^{PYTHIA}, presented in the right panel of Fig. 3. We find consistent ΔI_{AA}^{PYTHIA} for different values of R and constituent p_{T} threshold [16] (not shown). Within present experimental uncertainties, we do not observe significant redistribution of the jet energy.

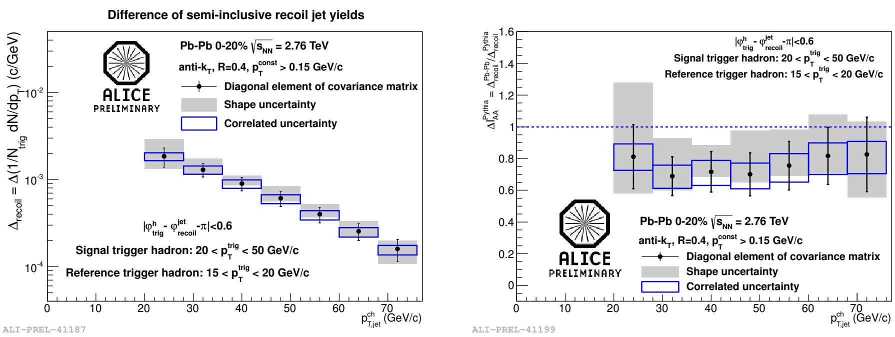

Figure 3: Semi-inclusive recoil jet spectrum difference Δ_{recoil} for 0-20% central collisions, $p_{\mathrm{T}}^{const} > 0.15$ GeV/c, jets reconstructed with anti-k_{T} for R=0.4 (left). Δ_{IAA} for recoil jets using PYTHIA as a reference (right).

References

1. M. Cacciari, G. P. Salam and G. Soyez, *Eur. Phys. J.* C **72**, 1896 (2012).
2. B. Abelev *et al.* [ALICE Collaboration], *arXiv:1301.3475 [nucl-ex]*.
3. N. Armesto, private communication.
4. G. Soyez, *Phys. Lett.* B **698**, 59 (2011).
5. M. Vajzer [ALICE Collaboration] *arXiv:1212.6890 [nucl-ex]*.
6. G. Aad *et al.* [ATLAS collaboration], Phys. Rev. D 84, 054001 (2011).
7. S. K. Prasad [ALICE Collaboration] *J. Phys. Conf. Ser.* **389**, 012005 (2012).
8. R. Ma [ALICE collaboration] *arXiv:1208.4537 [nucl-ex]*.
9. T. Sjostrand, S. Mrenna and P.Z. Skands, *JHEP* **05**, 026 (2006).
10. S. Roesler, R. Engel and J. Ranft, Lisbon 2000 - Advanced Monte Carlo (2000), 1033-1038 *arXiv:0012252 [hep-ph]*.
11. R. Reed [ALICE collaboration] *arXiv:1304.5945 [nucl-ex]*.
12. S. Aiola [ALICE collaboration] *arXiv:1304.6668 [nucl-ex]*.
13. M. Verweij [ALICE Collaboration] *arXiv:1208.8264 [nucl-ex]*.
14. M. Verweij [ALICE Collaboration] *arXiv:1208.6169 [nucl-ex]*.
15. B. Abelev *et al.* [ALICE Collaboration], *arXiv:1301.4361 [nucl-ex]*.
16. L. Cunqueiro [ALICE Collaboration] *arXiv:1210.7610 [nucl-ex]*.